REPORT DOCUMENTATION PAGE

Form Approved
OMB No. 0704-0188

1. REPORT DATE *(DD-MM-YYYY)*	2. REPORT TYPE	3. DATES COVERED *(From - To)*
1/8/07	FINAL	4/15/05 to 10/14/06

4. TITLE AND SUBTITLE
DURIP: Few-cycle Optical Parametric chirped Pulse Amplification

5a. CONTRACT NUMBER

5b. GRANT NUMBER
FA9550-05-1-0281

5c. PROGRAM ELEMENT NUMBER

6. AUTHOR(S)
Franz X. Kaertner

5d. PROJECT NUMBER

5e. TASK NUMBER

5f. WORK UNIT NUMBER

7. PERFORMING ORGANIZATION NAME(S) AND ADDRESS(ES)

Research Laboratory of Electronics
Massachusetts Institute Of Technology
77 Massachusetts Avenue
Cambridge, MA 02139

8. PERFORMING ORGANIZATION REPORT

9. SPONSORING / MONITORING AGENCY NAME(S) AND ADDRESS(ES)

AFOSR
875 North Randolph Street
Arlington, VA 22203

10. SPONSOR/MONITOR'S ACRONYM(S)
AFOSR

11. SPONSOR/MONITOR'S REPORT NUMBER(S)

12. DISTRIBUTION / AVAILABILITY STATEMENT
No restrictions

DISTRIBUTION STATEMENT A
Approved for Public Release
Distribution Unlimited

13. SUPPLEMENTARY NOTES

14. ABSTRACT
See attached

15. SUBJECT TERMS

16. SECURITY CLASSIFICATION OF:			17. LIMITATION OF ABSTRACT	18. NUMBER OF PAGES	19a. NAME OF RESPONSIBLE PERSON
a. REPORT	b. ABSTRACT	c. THIS PAGE		15	Franz X. Kaertner
					19b. TELEPHONE NUMBER *(include area code)* 617-452-3616

Standard Form 298 (Rev. 8-98)
Prescribed by ANSI Std. Z39.18

Final Report for DURIP 2005: FA9550-05-1-0281

Few-Cycle Optical Parametric Chirped Pulse Amplification

Franz X. Kärtner
Department of Electrical Engineering and Computer Science
and Research Laboratory of Electronics
Massachusetts Institute of Technology
Cambrdige, MA 02319

Summary:
Over the last few years, ultrafast laser physics and frequency metrology has merged and provided us with unprecedented (sub-cycle) control over the electric field of few-cycle laser pulses emitted from modelocked lasers.

These pulses and the corresponding technology are the prerequisite for high energy phase controlled few-cycle laser pulses, needed for reliable extreme ultraviolet (EUV) and soft x-ray production via high harmonic generation. It has been shown over the last few years that this technology leads to the generation of attosecond pulses and therefore opens up a new frontier in time and frequency measurements.

The DURIP funding provided by AFOSR enabled us to buy the key components for the construction of phase controlled high energy optical parametric chirped pulse amplifiers that directly generate two-cycle optical pulses, i.e. 14fs at a center wavelength of 2μm and later also of 5fs at 800nm at 1kHz repetition rate without using external pulse compression. The major challenge is the construction of a high beam quality pump source and the dispersion compensation of the ultra wideband spectrum after amplification. We want to use this source for soft x-ray production via high harmonic harmonic generation (HHG) and later attosecond pulse generation. Furthermore, this system enables us to explore in the future few and single-cycle laser pulse generation over the wavelength range covering 700nm – 2.6μm. Unlike Ti:sapphire amplifiers, parametric amplification is not limited to a fixed wavelength range. Therefore, this system will enable us to explore few-cycle pulse generation from the visible to the far infrared enabling many experiments to come over the next years. In particular, this system once finalized over the next half year will be used in the DARPA funded project "Hyperspectral Radiography Sources using Cavity-Enhancement Techniques". One immediate experiment we want to explore is to study HHG as a function of the drive laser wavelength. It is expected that the cutoff wavelength of high harmonics scales as the square of the wavelength, because the wiggler energy of the freed electron scales with the wavelength at fixed intensity. This scaling, if successful, could allow the generation of keV radiation using high-order harmonic generation. Of course, many other yet unconsidered effects might change this simple scaling, such as higher absorption or larger phase mismatch at these higher frequencies scaling with the driver pulse wavelength. In the following, we describe in detail what has been accomplished over the last 1.5 years supported by the DURIP funding and the future experimental work using the constructed laser source.

1. Parametric chirped-pulse amplification of difference-frequency generation

The complete setup under construction for generating intense CE-phase-stable two-cycle 2μm driving pulses for long-wavelength high-harmonic generation is shown in Fig. 1.

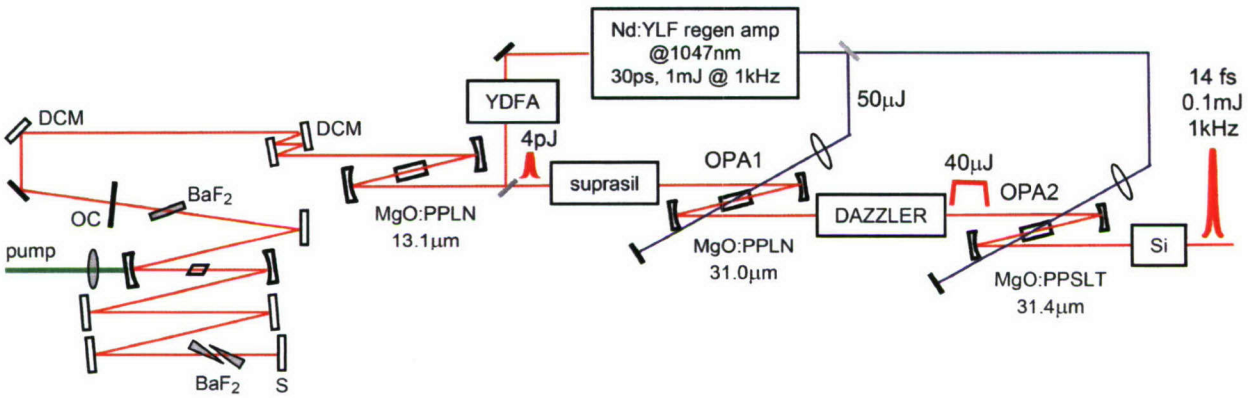

Figure 1. Schematic of optical setup for generating CE-phase-stable, 14fs, 0.1mJ laser pulses. Infrared pulses (1.6-2.4μm) obtained by difference-frequency mixing of octave-spanning Ti:sapphire pulses in a MgO:PPLN crystal, are amplified from 4pJ in two OPA stages to 0.1mJ. Synchonization of the 30ps Nd:YLF regenerative amplifier is accomplished by seeding with 1047nm light from the laser oscillator pre-amplified in a Yb-doped fiber amplifier. The stretcher-compressor unit can be implemented using bulk suprasil300 and silicon blocks and an IR DAZZLER.

The system consists of an octave spanning Ti:sapphire laser that can be directely carrier-envelope phase stabilized. This is important if later parametric chirp pulse amplification of these all ready phase stabilized pulses is pursued using a 532 nm pump laser. Here, we used the broadband output of the laser to generate directly phase stable pulses by difference frequency generation in a MgO:PPLN with a poling period of 13.1 μm to generate a broadband 2 μm seed pulse. After the DFG generation the 1030 nm fundamental spectrum is preamplified in a fiber amplifier to seed a Nd:YLF regenerative amplifier that provides the pump pulses for the following optical parametric chirped pulse amplification (OPCPA) stages. The seed pulses are stretched in a block of suprasil to about 20ps length and preamplified in OPA1. After the first stage, when enough signal amplification has occurred, an infrared DAZZLER is used for pulse shaping and higher order dispersion compensation. Then the pulses are amplified to the >0.1mJ level in a second OPCPA stage and compressed in a silicon block. Note, this is a very compact layout for stretching and compression using bulk media and a DAZZLER only. In the following sections, we discuss the individual components of the setup in detail.

2. Generation of two-cycle signal pulses with carrier-envelope phase stabilization

Over the past two years, we have demonstrated an f-to-2f self-referenced, octave-spanning 200 MHz Ti:sapphire laser with only 50 attosecond carrier-envelope (CE) phase jitter,[2] the experimental setup is shown in Fig. 2.

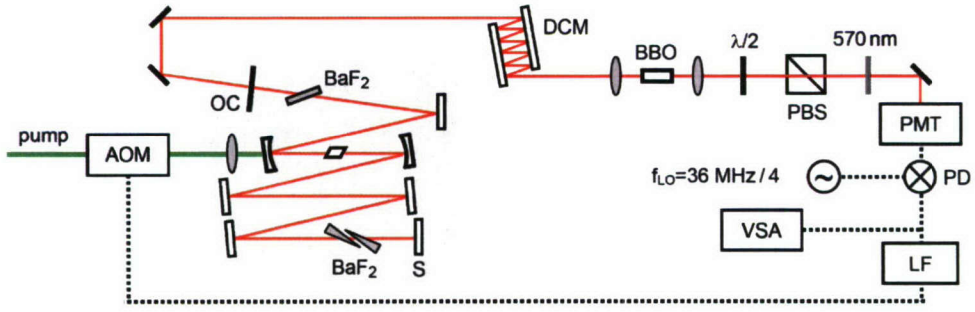

Figure 2. CE-phase stabilized 200 MHz octave-spanning Ti:sapphire laser. The femtosecond laser itself (located inside the grey area) has a compact 20 cm×30 cm footprint. AOM, acousto-optical modulator; S, silver end mirror; OC, output coupling mirror; PBS, polarizing beam splitter cube; PMT, photomultiplier tube; PD, phase detector; LF, loop filter; VSA, vector signal analyzer. The CE frequency is phase locked to 36 MHz.

These prismless Ti:sapphire lasers require no realignment over many days of operation and no major realignment over weeks of operation. The long-term stability of this source is of major importance for constructing and operating more complex laser systems as intended in this project. The output spectrum of the Ti:sapphire laser is depicted in Fig. 3.

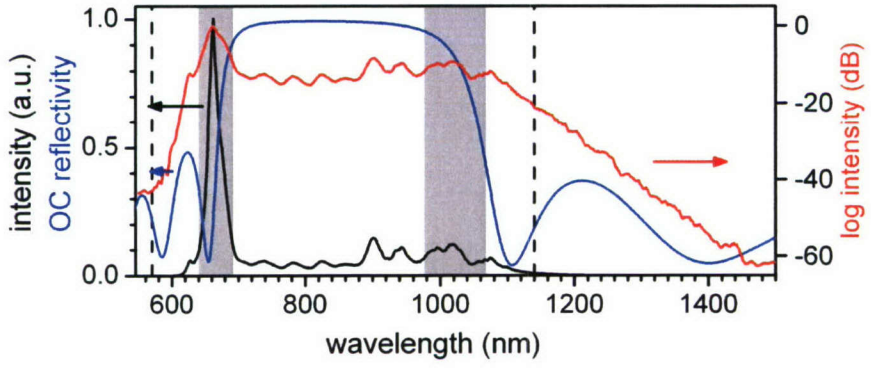

Figure 3. Output spectrum of the Ti:sapphire laser on a linear (black curve) and on a logarithmic scale (red curve). The reflectivity of the ZnSe/MgF_2 output coupler (blue curve) is shown for comparison. The Fourier limit of the pulse spectrum is 3.6 fs. The wavelengths 570 and 1140 nm used for f-to-2f self-referencing are indicated by two dashed lines. The spectral components highlighted by the grey areas contribute to the infrared pulse generation by difference-frequency mixing (see Fig. 9).

Key issues for generating such ultrabroadband spectra directly from the laser oscillator are (a) precise dispersion compensation using double-chirped mirror (DCM) pairs and BaF_2 plates and wedges for dispersion fine-tuning, (b) spectral shaping of the output using a custom-designed ZnSe/MgF_2 output coupling mirror (see blue curve in Fig. 3) for enhancing the spectral wings (prerequisite for f-to-2f self-referencing and difference-frequency generation (DFG) to 2μm), and (c) a thorough understanding of the pulse shaping dynamics and optimization of the Kerr-lensing action.

Using f-to-2f self-referencing with the 1140nm and 570nm spectral components directly from the laser output, we achieved an ultralow CE phase jitter of only 50 as at a wavelength of 800 nm (see Fig. 4). This record-low CE phase jitter is essential for many applications in CE-phase-

sensitive time-domain spectroscopy[3, 4] and in attosecond X-ray pulse generation[5]. In addition, we investigated the CE phase dynamics of octave-spanning Ti:sapphire lasers and performed a complete noise analysis of the CE phase stabilization.[6] The effect of the laser dynamics on the residual CE phase noise was modeled by deriving a transfer function representation of the octave-spanning frequency comb. The modelled phase noise and the experimental results show excellent agreement (not shown). This greatly enhances our capability of predicting the dependence of the residual CE phase noise on the feedback loop filter, the CE frequency control mechanism and the pump laser used.

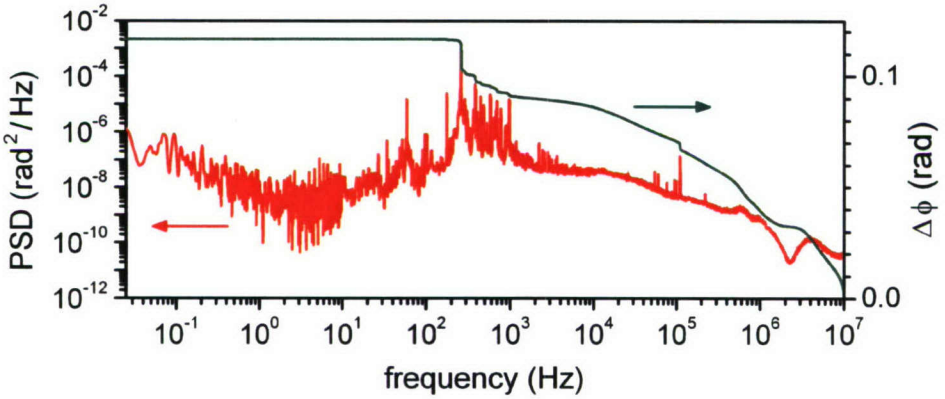

Figure 4. CE-phase noise power-spectral density (red curve) and integrated residual (rms) CE phase error (green curve) measured using an analog mixer as phase detector (PD in Fig. 1). The measured in-loop CE phase error of 0.117 rad is equivalent to only 50 attosecond CE phase jitter at 800 nm.

During the past two years our group has also made significant progress in single-cycle pulse generation by coherent pulse synthesis[7] from a 5-fs Ti:sapphire (Ti:sa) laser and a 20-fs Cr:forsterite (Cr:fo) laser (see Fig. 5).[8]

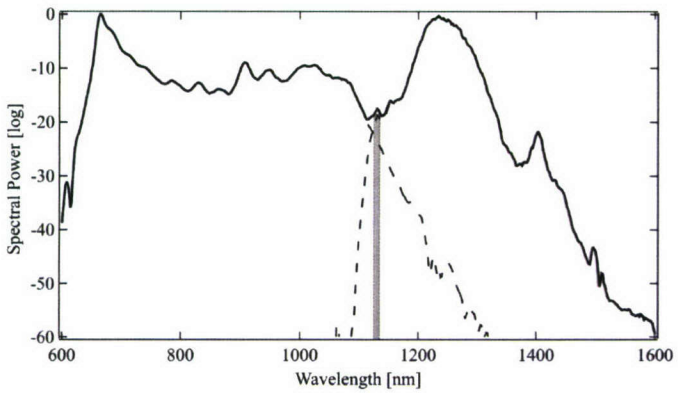

Figure 5. Optical spectra of the mode-locked Ti:sapphire and Cr:forsterite laser. The dashed lines indicate the spectra of the individual lasers in the vicinity of the spectral overlap, and the shaded region indicates the spectral region used to detect the difference in CE frequency between the two lasers.

The spectrum of the Ti:sa laser overlaps with the spectrum of the Cr:fo laser. Coherent superposition of the Ti:sa laser pulses with the Cr:fo laser has been achieved due to the enhanced stability of their prismless cavities. The most important and critical step is long-term stable and tight synchronization of the repetition rates of both lasers[9] which has been achieved using a balanced cross-correlation technique (see Fig. 6). An analysis of the out-of-loop timing jitter following Ref. [9] shows that the rms jitter measured in a 2.3 MHz BW results in 380 as ±130 as,[10] a tenth of an optical cycle at the center wavelength of the joint Ti:sa-Cr:fo spectrum of

~950 nm. This performance can be maintained over more than 12 hours of continued operation, which demonstrates the stability of the system.

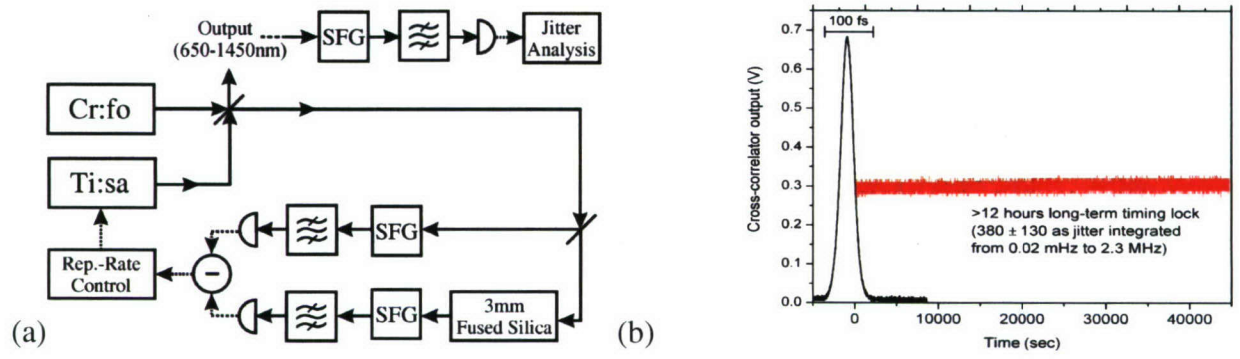

Figure 6: (a) Experimental setup of the synchronized lasers. Cr:fo: passively mode-locked Cr:forsterite laser, Ti:sa: passively mode-locked Ti:sapphire laser; SFG: sum-frequency generation; all bandpass filters transmit only the sum-frequency (1/496nm = 1/833nm+1/1225nm). The two beam splitters consist of a thin fused silica substrate coated with a semi-transparent metal film. The third correlator is used to generate the graph shown in (b), which shows the timing jitter determined from the amplitude noise of the SFG from the out-of-loop cross-correlator. The trace is shown over 12 hours of continuous operation without interruption and the relative timing jitter is about a tenth of an optical cycle, i.e., 300as at 1μm wavelength. The lock was intentionally broken after 12hours.

Rather recently, we have demonstrated the generation of a phase-coherent spectrum[11] from ultrabroadband Ti:sa and Cr:fo lasers from 600 nm to 1500 nm by locking the difference in the CE phase between the two lasers to a local oscillator (Fig. 7).

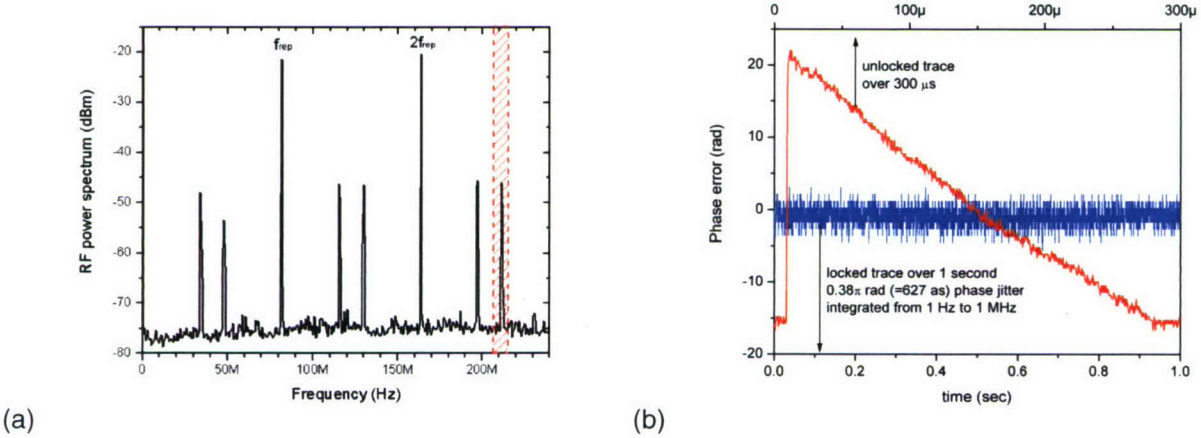

Figure 7: (a) RF spectrum (RBW 30 kHz) of the beat signals from the APD output. Red shadowed region indicates the bandpass filter centered at 215 MHz that selects the beat signal used for phase-locking. (b) In-loop phase error signal from the digital phase detector. Red curve shows the free-running phase error signal over 300 μsec time scale. Blue curve shows the residual in-loop phase error for 1 second when it is locked. The residual phase jitter from 1 Hz to 1 MHz is 0.38π rad (equivalent to 627 attoseconds at the center wavelength of 1 μm).

3. CE-phase-stable seed pulses at 2μm from difference-frequency generation

In order to generate the infrared seed pulses for optical parametric chirped-pulse amplification (OPCPA) at 2μm, the output pulses of the Ti:sapphire are focused into a 3mm long MgO-doped periodically-poled lithium niobate (PPLN) crystal with a poling period of 13.1 μm (see Figs. 1

and 8), in which difference-frequency mixing of the laser spectrum creates the ultrabroadband spectrum extending from 1.6-2.4 μm shown in Fig. 9. The pulse energy of the DFG pulses is in the few pJ range, the spectrum corresponds to a ~14fs, two-cycle pulse at a center wavelength of 2μm.

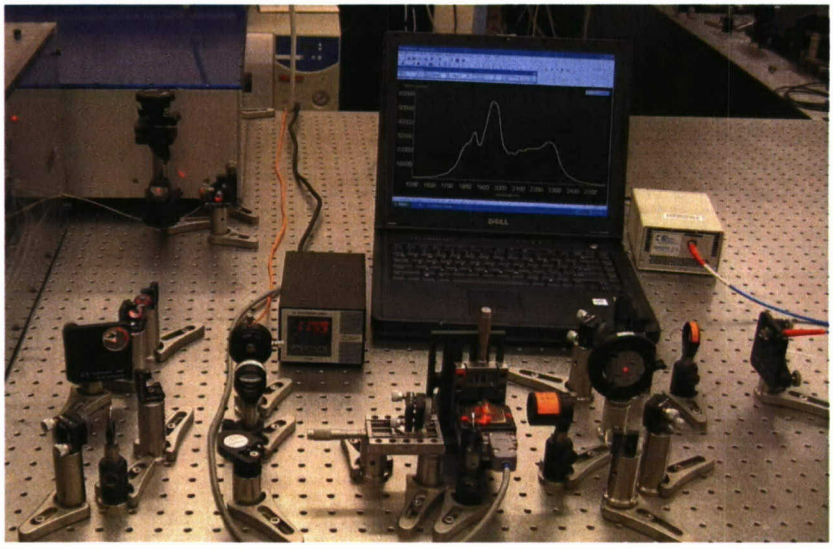

Figure 8. Experimental setup for broadband DFG (1.6-2.4μm). The Ti:sapphire laser is inside the plexiglas box on the LHS, the Nd:YLF regenerative amplifier can be seen in the upper left corner. In the forefront, the MgO:PPLN crystal heated to 120°C in a temperature-controlled oven can be seen.

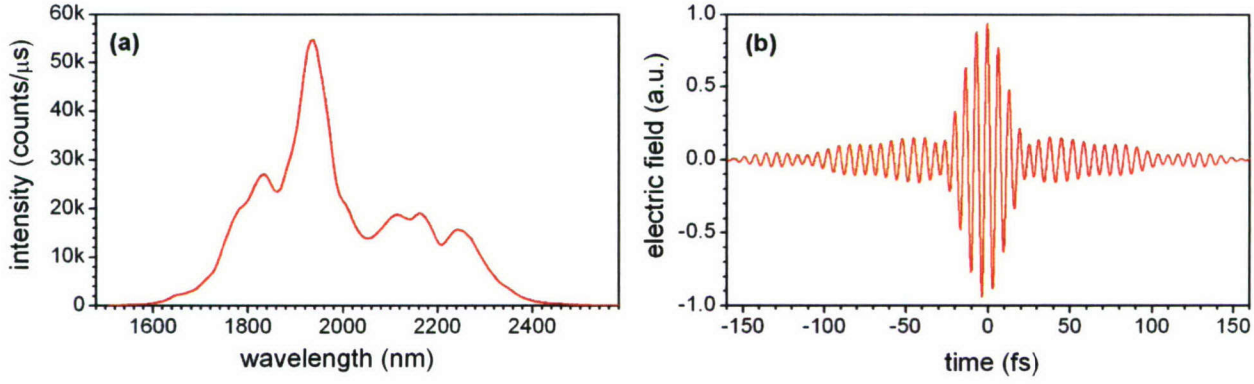

Figure 9: (a) Measured DFG spectrum obtained by difference-frequency mixing of octave-spanning Ti:sapphire pulses (shown in Fig. 2) in a MgO:PPLN crystal. (b) Electric field versus time calculated from the spectrum under the assumption of a flat spectral phase. This electric field corresponds to a DFG pulse duration of ~14fs or approximately two optical cycles at 2μm assuming perfect dispersion compensation

Note that, because the infrared light at 2μm is created by difference-frequency generation, the seed pulses for the OPCPA automatically possess a stable CE phase.[12, 13]

4. Stretcher and compressor setup for two-cycle signal pulses

To ensure efficient energy transfer from the pump to the signal (i.e., seed) pulses, a stretcher-compressor unit is needed to match the temporal duration of the signal pulses with that of the

pump pulses. For 30-ps pump pulses and 14-fs signal pulses, this corresponds to a stretching factor of ~2000.

We have designed an ultracompact stretcher-compressor unit employing a Brewster-cut 150 mm suprasil300 glas block, a programmable acousto-optic dispersion filter (DAZZLER from Fastlite) based on a 45mm TeO_2 crystal, and a 30mm silicon block for compression. As the DFG pulse energy is in the few pJ range, we first stretch the pulses almost lossless in 150 mm suprasil300 in front of the first OPA stage. Placing the DAZZLER, which has a diffraction efficiency of only ~10%, in between the first and second OPA stages has the advantage to reduce problems arising from amplified spontaneous emission (ASE) in the first OPA stage due to the low seed pulse energy.[14] Because we do not employ gratings or prisms, we expect this stretcher-compressor unit to be very stable with respect to beam pointing instabilities.

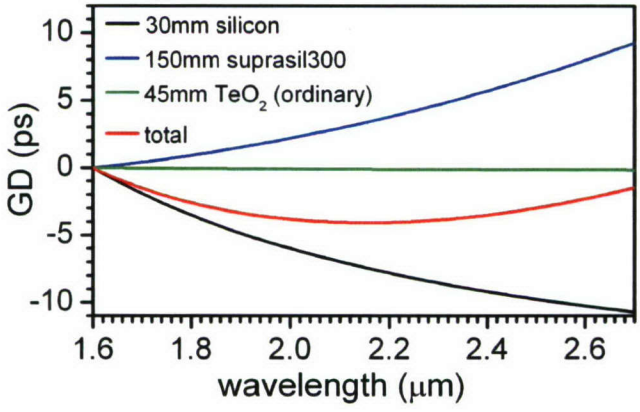

Figure 10. Stretcher-compressor unit: group delay (GD) of 30mm silicon, 150mm suprasil300, 45mm TeO_2 (DAZZLER) for ordinary axis (extraordinary axis indistinguishable within line width), and resulting total group delay of the stretcher-compressor unit. From the Sellmeier equations of TeO_2, the programmable maximum group delay in this wavelength range is larger than 20ps, thus the group delay can precisely be compensated over the full spectrum of the DFG pulses shown in Fig.9.

5. Synchronization of signal and pump pulses

Synchronization of pump and signal pulses in the two OPA stages is a crucial requirement since any temporal mismatch directly affects the parametric process, reducing its efficiency and distorting the signal pulse.

Synchronization between the Ti:sapphire laser and Nd:YLF regenerative amplifier is accomplished by injection seeding of the amplifier[15]: After the DFG setup (see Figs. 7-8), we couple ~120μW (within 10nm at 1050nm) into an optical fiber using an angled-body fiber collimator. Because this is not enough power to seed the regenerative amplifier, we first amplify it to 1.2mW (within the same bandwidth) using a home-built Yb-doped fiber amplifier (YDFA, see Figs. 1 and 11). This is enough to overcome the ASE within the 0.05 nm bandwidth (minimum bandwidth for a 30-ps pulse) centered at 1047 nm. This all-optical synchronization scheme reduces the complexity and cost of the entire system, ensures low timing jitter, and allows hassle-free OPCPA.

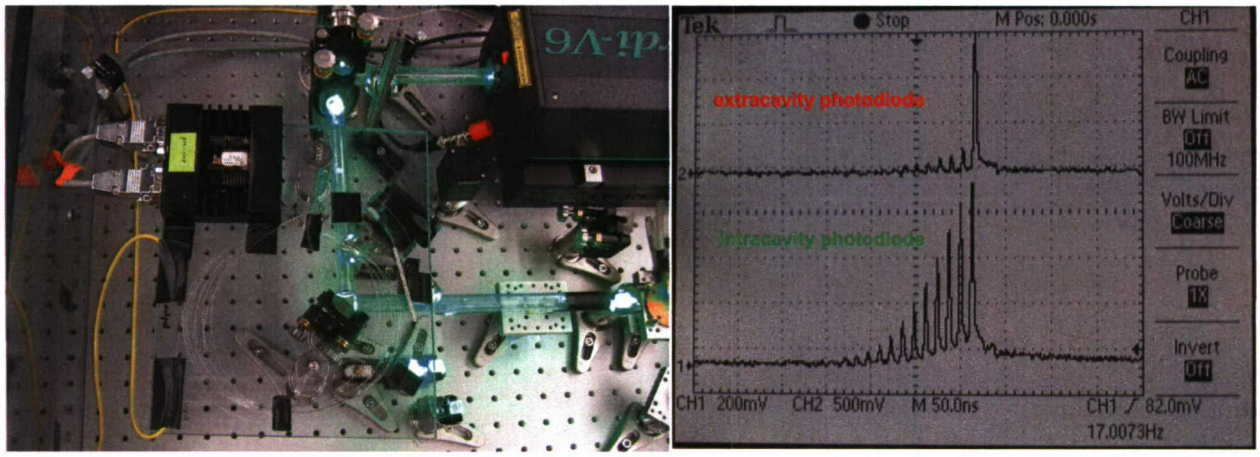

Figure 11. (Left) Custom-built Yb-doped fiber amplifier (YDFA) located inside the plexiglas box of the Ti:saphhire laser. (Right) Seeding of the Nd:YLF regenerative amplifier with 1047nm light from the Ti:sapphire laser amplified in the YDFA. The intracavity photodiode shows the build-up of pulse energy, the extacavity photodiode shows the amplified pulse switched out of the cavity and a few post pulses exhibiting much smaller energy.

However, synchronization between the Ti:sapphire laser and Nd:YLF regenerative amplifier is only one part of the whole synchonization scheme (see Fig. 12) consisting of synchronizing the Ti:sapphire laser, the Nd:YLF amplifier, and the DAZZLER.

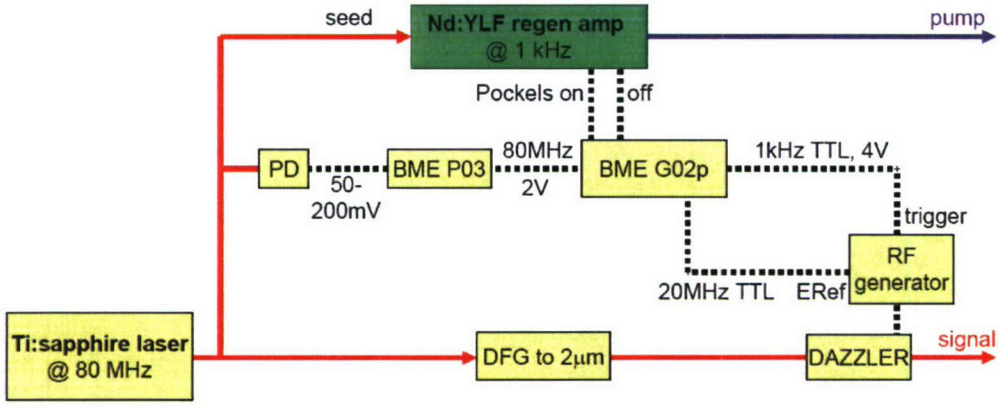

Figure 12. Electronics scheme for synchronizing the Ti:sapphire laser, the Nd:YLF amplifier, and the DAZZLER.

The 80 MHz repetition rate of the Ti:sapphire laser is detected using a fast photodiode (PD). The PD signal is then preamplified using a resonant preamplifier BME P03 (from Bergmann Meßgeräte Entwicklung, Germany). A Digital Delay/Pulse Generator BME G02p picks every 80.000 pulse from the Ti:sapphire pulse train and sends trigger pulses, which can be delayed/advanced by up to 1 ms, to the Nd:YLF amplifier (Pockels cell on/off) and to the RF generator of the DAZZLER. In addition, the BME G02p provides the 20MHz reference signal for the RF generator.

6. Optical parametric chirped pulse amplification of two-cycle pulses

In the past few years, optical parametric chirped pulse amplification (OPCPA) has emerged as an attractive alternative to stimulated-emission based amplifier systems. The main advantages of

OPCPA are large single-pass parametric gain, large 'engineerable' gain bandwidth supporting few-cycle pulses, absence of thermal loading problems, and – very important - the CE phase is preserved during the OPCPA process.[14, 16, 17]

In parametric amplification, pump photons are converted into two lower frequency photons (signal and idler) when seeded by photons at the signal wavelength and satisfy the (energy-conservation) relation:

$$\omega_p \rightarrow \omega_s + \omega_i,$$

where ω_p, ω_s, and ω_i are the pump, signal (seed), and idler frequencies, respectively. In addition these three waves must be phase matched (momentum conservation),

$$\Delta k = k_p - k_s - k_i,$$

where k_p, k_s, and k_i are the wave vectors for pump, signal, and idler, respectively. Δk is the wave-vector mismatch. In our experiment, using MgO:PPLN and MgO:PPSLT as nonlinear materials results in ultra broadband quasi-phase matching (i.e., $\Delta k \approx 0$, see Fig. 13) because of near-degeneracy pumping with a 1047nm pump source. Meanwhile, multi-grating chips of these materials have been fabricated by HCPhotonics and are now ready to be used in our experiment.

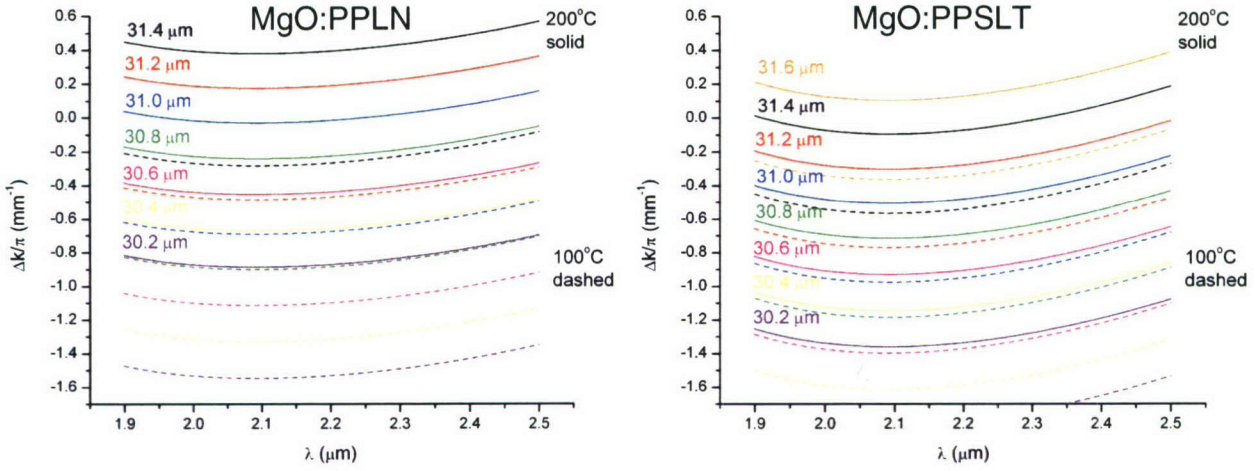

Figure 13. Quasi-phase matching with (left) MgO:PPLN and (b) MgO:PPSLT for different poling periods indicated on the LHS and two different temperature (200°C solid curves, 100°C dashed curves). The wave-vector mismatch can continuously be adjusted by varying the temperature between 100°C and 200°C.

7. Few-cycle pulse characterization

The process of high-harmonic generation (HHG), for which the OPCPA-of-DFG-source shown in Fig. 7 is built, is highly sensitive to the intensity and duration of the driving pulse. The spatial properties of the XUV beam are highly sensitive to the spatio-temporal structure of the driving field.[18] For example, the spatial profile of the driving beam can be used to control the focusing of the XUV beam.

In the past two years, we have developed a pulse characterizaton method called two-dimensional spectral shearing interferometry (2DSI).[19] This technique does not suffer from the calibration sensitivities of SPIDER nor the bandwidth limitations of FROG or interferometric

autocorrelation (IAC).[20] In 2DSI, two chirped (quasi-CW) pulse copies are mixed with the short pulse to be measured in a type II $\chi^{(2)}$ crystal (see Fig. 14).

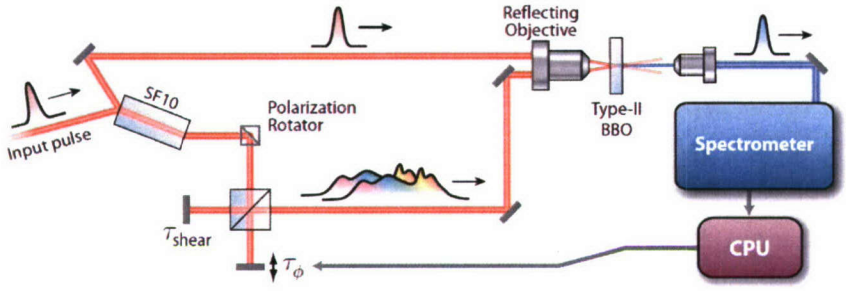

Figure 14. Setup for two-dimensional spectral shearing interferometry (2DSI).

The advantage of type II upconversion with BBO is that the phase matching bandwidth is large in one axis (well over an octave) and small in the other, a perfect match for single-cycle pulse characterization. Furthermore, self-referenced frequency shifting roughly halves the relative bandwidth of the final signal allowing the measurement of pulses spanning 2 octaves from 700 nm to 2800 nm.

The two up-converted pulses are sheared spectrally, but are collinear forming a single pulse in time. The zeroth-order phase of one of the up-converted pulses is scanned over several cycles by vibrating the corresponding mirror in the interferometer a few microns. The spectrum of the up-converted signal is recorded as a function of phase delay and wavelength, yielding a 2D intensity function, see Fig. 15(a) and (b). Since only the relative fringe phase matters, the delay scan does not need to be calibrated in any way, the only required calibration is for the shear a relatively insensitive parameter.[21, 22]

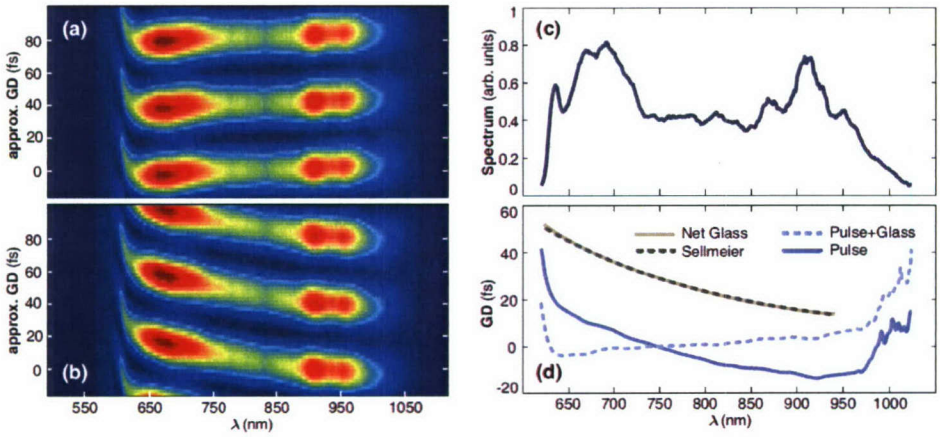

Figure 15: Few-cycle pulse characterization: Measured raw 2DSI traces for pulse (a) before and (b) after dispersion by glass plate; (c) Measured optical spectrum; (d) extracted phase difference (dashed) and theoretical (solid) prediction for fused silica; (d) phase delay error computed from (c).

We used this method to characterize a 5 fs pulse from one of our Ti:sapphire lasers both before and after dispersion from a 1 mm fused silica plate,[19] see Fig. 15(a), along with the extracted spectral group delays. The chirp introduced by the glass plate is reflected in the measurement with high precision demonstrating the high quality of pulse reconstruction achieved with this method.

In the coming months, we plan to extend this method to a complete spatio-temporal characterization of the pulse: Due to the collinear nature of the measurement, the fringe shown

above is available at *each* point in the transverse beam profile. This will result in a 4D data set (a 2D fringe like that in Fig. 13(a) obtained at each transverse spatial coordinate) from which the spectral group delay can be obtained at each point in the beam enabling a complete spatio-temporal characterization of the pulse.

While other methods have been demonstrated that are capable of full 3D measurement, 4DSI, if successful, will be the first method capable of measuring the full spatio-temporal characteristics of pulses below 1 ps,[23] and should nonetheless be capable of measuring single-cycle pulses.

8. Long-wavelength high-harmonic generation

In the coming months, we want to employ the amplified few cycle 2μm pulses from the source shown in Fig. 1 for studying the long-wavelength scaling behavior of high-harmonic generation (HHG). The desire for using longer wavelength driver pulses is motivated by the scaling of the HHG single-atom response. The HHG photon energy increases quadratically with the driver pulse wavelength and linearly with its intensity, according to the following equation[24]:

$$\hbar\omega_{\max} = I_p + 3.17\frac{E_0^2 e^2}{4m\omega_D^2}$$

where $\omega_{\max}$ is the highest achievable harmonic energy, e and m are the electron charge and mass, and E_0 and ω_D are the driver field amplitude and frequency.

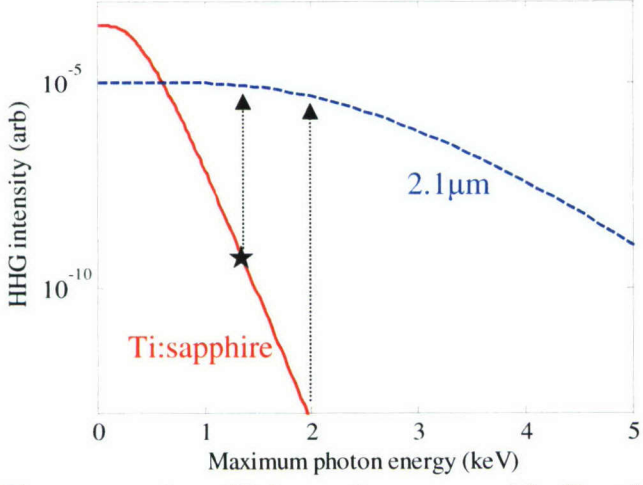

Figure 16: Scaling of the single atom HHG photon yield with the maximal achievable photon energy. Ti:sapphire driver pulses (red solid line) can hardly reach 1 keV. In the keV region, 2.1μm driver pulses (blue dashed) outperform them by many orders of magnitude. The star shows the location of the experiment that reached the record photon energy[1] on the yield curve.

The conversion efficiency decreases cubically with the drive wavelength and *exponentially* with the intensity.[25] The state-of-the-art experimental systems,[1] where high photon energies are obtained by simply increasing the intensity of the driver pulses (at 720nm), already lie in *the exponential tail of the efficiency curve* (see Fig. 16). This has been shown in a recent study in our group.[25] By using longer wavelength driver pulses the exponential falloff of the efficiency is pushed to much higher photon energies, as Fig. 16 demonstrates. Experimental studies of HHG with longer wavelength driver pulses are very few,[26, 27] and the experimental performance was limited by the pulse intensity and duration constraints rather than by the HHG process itself.

Thus this work could result in a compact soft-X-ray source emitting few keV photons. Whether this hypothesis is true needs to be checked experimentally. OPCPA is at the moment the only technique to deliver high energy pulses at both wavelength ranges, i.e., 0.8 μm and 2 μm.

9. Attosecond pulse generation

Recently, it has been demonstrated by the Vienna group that attosecond pulses can be generated by exploiting the spectral dependence of the high-harmonic generation on the CE phase of the femtosecond pulse that generated these harmonics[28] and first time-resolved studies using those pulses are reported.[29] Even more recently, the reproducible generation of these attosecond pulses from shot to shot has been achieved by phase control of the high energy laser pulses.[5] For a 5 fs high-energy pulse, see Figure 17, with zero CE phase, the resulting electric field is symmetric and leads to an emission of a single attosecond pulse in the cut-off region of the harmonics, in contrast to its antisymmetric counter part for a CE phase of $\phi_{CE} = \pi/2$. In the absence of a stabilization and control of the CE phase, no isolated attosecond pulse is generated. As a consequence, reproducible production of sub-femtosecond X-ray pulses rely on driver pulses with reproducible CE phase in addition to a well-determined intensity envelope.

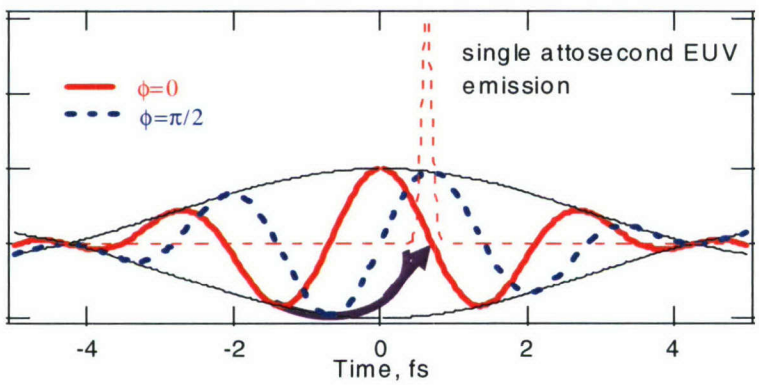

Figure 17: Phase controlled few-cylce laser pulses and single attosecond EUV emission by high-harmonic generation for the even pulse.

The generated attosecond pulse together with the tightly correlated few-cycle driver pulse enables time-resolved spectroscopy on an attosecond time scale. The effect of the electromagnetic pulse on the photoelectrons released by an x-ray pulse is well understood by now.[30, 31] First the photoelectron is created by a short x-ray pulse with a distribution of initial momenta known from conventional photo-ionization models. Second the photoelectron is subsequently accelerated as a classical particle by the electric field of the phase-controlled few-cycle pulse. The model predicts that, depending on the oscillation phase of the light field at the instant of creation of the electron, a momentum component along the electric field vector is added to the initial momentum of the electron, resulting in a shift of the photoelectron distribution up or down in momentum space. The momentum transfer gives rise to a change in the final kinetic energy of the photoelectrons collected within a finite solid angle as can be revealed by time-of–flight spectroscopy.[28] As a result of such measurements, the generated attosecond x-ray pulses can be completely characterized with respect to amplitude and phase.[31] These capabilities open up an exciting new frontier in ultrafast time-resolved experiments.

REFERENCES

[1] J. Seres, E. Seres, A. J. Verhoef, G. Tempea, C. Streli, P. Wobrauschek, V. Yakovlev, A. Scrinzi, C. Spielmann, and F. Krausz, "Source of coherent kiloelectronvolt X-rays," *Nature*, vol. 433, pp. 596, 2005.

[2] O. D. Mücke, R. Ell, A. Winter, J. Kim, J. R. Birge, L. Matos, and F. X. Kärtner, "Self-Referenced 200 MHz Octave-Spanning Ti:Sapphire Laser with 50 Attosecond Carrier-Envelope Phase Jitter," *Opt. Express*, vol. 13, pp. 5163, 2005.

[3] O. D. Mücke, T. Tritschler, M. Wegener, U. Morgner, F. X. Kärtner, G. Khitrova, and H. M. Gibbs, "Carrier-wave Rabi flopping: role of the carrier-envelope phase," *Opt. Lett.*, vol. 29, pp. 2160, 2004.

[4] C. Jirauschek, L. Duan, O. D. Mücke, F. X. Kärtner, M. Wegener, and U. Morgner, "Carrier-envelope phase-sensitive inversion in two-level systems," *J. Opt. Soc. Am. B*, vol. 22, pp. 2065, 2005.

[5] A. Baltuska, T. Udem, M. Uiberacker, M. Hentschel, E. Goullelmakis, C. Gohle, R. Holzwarth, V. S. Yakovlev, A. Scrinzi, T. W. Haensch, and F. Krausz, "Attosecond control of electronic processes by intense light fields," *Nature*, vol. 421, pp. 611, 2003.

[6] L. Matos, O. D. Mücke, J. Chen, and F. X. Kärtner, "Carrier-envelope phase dynamics and noise analysis in octave-spanning Ti:sapphire lasers," *Opt. Express*, vol. 14, pp. 2497, 2006.

[7] R. K. Shelton, L. S. Ma, H. C. Kapteyn, M. M. Murnane, J. L. Hall, and J. Ye, "Phase-coherent optical pulse synthesis from separate femtosecond lasers," *Science*, vol. 293, pp. 1286-1289, 2001.

[8] T. R. Schibli, O. Kuzucu, J.-W. Kim, E. P. Ippen, J. G. Fujimoto, F. X. Kaertner, V. Scheuer, and G. Angelow, "Toward single-cycle laser systems," *IEEE J. of Selected Topics in Quantum Electronics*, vol. 9, pp. 990-1001, 2003.

[9] T. R. Schibli, J. Kim, O. Kuzucu, J. T. Gopinath, S. N. Tandon, G. S. Petrich, L. A. Kolodziejski, J. G. Fujimoto, E. P. Ippen, and F. X. Kaertner, "Attosecond active synchronization of passively mode-locked lasers by balanced cross correlation," *Opt. Lett.*, vol. 28, pp. 947, 2003.

[10] J. Kim, J. Burnham, J. Chen, F. X. Kärtner, F. Ö. Ilday, F. Ludwig, H. Schlarb, A. Winter, M. Ferianis, and D. Cheever, "An Integrated Femtosecond Timing Distribution System for XFELs," presented at European Particle Accelerator Conference (EPAC) 2006,, Edinburgh, UK, 2006.

[11] J. Kim, T. R. Schibli, L. Matos, H. Byun, and F. X. Kärtner, "Phase-coherent spectrum from ultrabroadband Ti:sapphire and Cr:forsterite lasers covering the visible to the infrared," presented at Ultrafast Optics (UFO/HFSW), Nara, Japan, 2005.

[12] O. D. Mücke, O. Kuzucu, F. N. C. Wong, E. P. Ippen, F. X. Kärtner, S. M. Foreman, D. J. Jones, L.-S. Ma, J. L. Hall, and J. Ye, "Experimental implementation of optical clockwork without carrier-envelope phase control," *Opt. Lett.*, vol. 29, pp. 2806, 2004.

[13] S. M. Foreman, A. Marian, J. Ye, E. A. Petrukhin, M. A. Gubin, O. D. Mücke, F. N. C. Wong, E. P. Ippen, and F. X. Kärtner, "Demonstration of a HeNe/CH_4-based optical molecular clock,," *Opt. Lett.*, vol. 30, pp. 570, 2005.

[14] T. Fuji, N. Ishii, C. Y. Teisset, X. Gu, T. Metzger, A. Baltuška, N. Forget, D. Kaplan, A. Galvanauskas, and F. Krausz, "Parametric amplification of few-cycle carrier-envelope phase-stable pulses at 2.1μm," *Opt. Lett.*, vol. 31, pp. 1103, 2006.

[15] C. Y. Teisset, N. Ishii, T. Fuji, T. Metzger, S. Köhler, R. Holzwarth, A. Baltuška, A. M. Zheltikov, and F. Krausz, "Soliton-based pump–seed synchronization for few-cycle OPCPA," *Opt. Express*, vol. 13, pp. 6550, 2005.

[16] C. P. Hauri, P. Schlup, G. Arisholm, J. Biegert, and U. Keller, "Phase-preserving chirped-pulse optical parametric amplification to 17.3 fs directly from a Ti:sapphire oscillator," *Opt. Lett.*, vol. 29, pp. 1369-1371, 2004.

[17] A. Baltuska, "Toward a terawatt few-optical cycle driver laser for attosecond spectroscopy," presented at Ultrafast Phenomena, Niigata Japan, 2004.

[18] M. Schnürer, Z. Cheng, M. Hentschel, F. Krausz, T. Wilhein, D. Hambach, G. Schmahl, M. Drescher, Y. Lim, and U. Heinzmann, "Few-cycle-driven XUV laser harmonics: generation and focusing," *Appl. Phys B*, vol. 70, pp. S227, 2000.

[19] J. R. Birge, R. Ell, and F. X. Kärtner, "Two-dimensional spectral shearing interferometry for few-cycle pulse characterization," *Opt. Lett.*, vol. 31, pp. 2063, 2006.

[20] L. Gallmann, D. H. Sutter, N. Matuschek, G. Steinmeyer, and U. Keller, "Techniques for the characterization of sub-10-fs optical pulses: a comparison," *Appl. Phys. B*, vol. 70, pp. S67, 2000.

[21] C. Iaconis and I. Walmsley, "Self-referencing spectral interferometry for measuring ultrashort pulses," *IEEE J. of Quantum Electronics*, vol. 35, pp. 501.

[22] C. Iaconis and A. Walmsley, "Spectral phase interferometryfor direct electric-field reconstructionof ultrashort optical pulses," *Opt. Lett.*, vol. 23, pp. 792, 1998.

[23] P. Gabolde and R. Trebino, "Self-referenced measurement of the complete electric field of ultrashort pulses," *Opt. Express*, vol. 12, pp. 4423, 2004.

[24] M. Lewenstein, P. Balcou, M. Y. Ivanov, A. L'Huillier, and P. B. Corkum, "Theory of high harmonic generation by low-frequency laser fields," *Phys. Rev. A*, vol. 49, pp. 2117, 1994.

[25] A. Gordon and F. X. Kärtner, "Scaling of keV HHG photon yield with drive wavelength," *Opt. Express*, vol. 13, pp. 2941, 2005.

[26] B. Sheehy, J. D. D. Martin, L. F. DiMauro, P. Agostini, K. J. Schafer, M. B. Gaarde, and K. C. Kulander, "High Harmonic Generation at Long Wavelengths," *Phys. Rev. Lett.*, vol. 83, pp. 5170, 1999.

[27] B. Shan and Z. Chang, "Dramatic extension of the high-order harmonic cutoff by using a long-wavelength driving field," *Phys. Rev. A*, vol. 65, pp. 011804(R), 2002.

[28] H. Hentschel, R. Kienberger, C. Spielmann, G. A. Reider, N. Milosevic, T. Brabec, P. Corkum, U. Heinzmann, M. Drescher, and F. Krausz, "Attosecond metrology," *Nature*, vol. 414, pp. 509-513, 2001.

[29] M. Drescher, H. Hentschel, R. Kienberger, M. Uiberacker, V. Yakoviev, A. Scrinzi, T. Westerwalbesloh, U. Kleineberg, U. Heinzmann, and F. Krausz, "Time-resolved atomic inner-shell spectroscopy," *Nature*, vol. 419, pp. 803-807, 2002.

[30] M. Drescher, M. Hentschel, R. Kienberger, G. Tempea, C. Spielmann, G. A. Reider, P. B. Corkum, and F. Krausz, "X-ray pulses approaching the attosecond frontier," *Science*, vol. 291, pp. 1923-1927, 2001.

[31] J. I. F. Quere, G. L. Yudin and P. B. Corkum, "Attosecond Spectral Shearing Interferometry," *Phys. Rev. Lett.*, vol. 90, pp. 073902-1, 2003.